

pH-Induced Changes in the Fabrication of Multilayers of Poly(acrylic acid) and Chitosan: Fabrication, Properties, and Tests as a Drug Storage and Delivery System

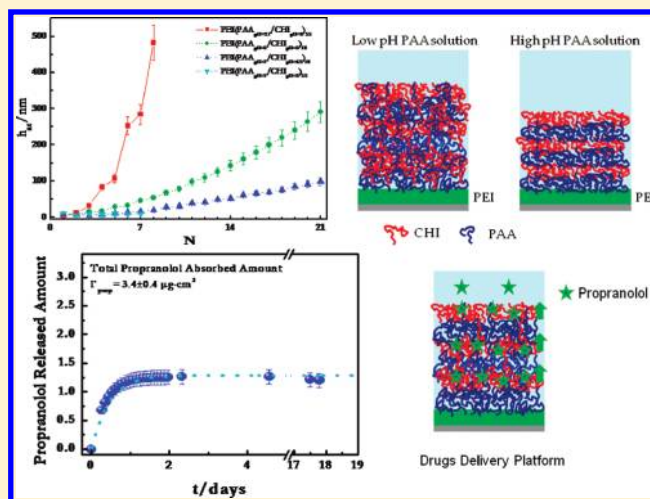
Eduardo Guzmán,^{†,§} Jesica A. Cavallo,[‡] Raquel Chuliá-Jordán,[†] César Gómez,[‡] Miriam C. Strumia,^{*,‡} Francisco Ortega,[†] and Ramón G. Rubio^{*,†}

[†]Departamento de Química Física I, Facultad de Ciencias Químicas, Universidad Complutense de Madrid, Ciudad Universitaria s/n, 28040-Madrid, Spain

[‡]Departamento de Química Orgánica, Facultad de Ciencias Químicas (IMBIV-CONICET), Universidad Nacional de Córdoba, Medina Allende esquina Haya de la Torre, Ciudad Universitaria, CP5000-Córdoba, Argentina

S Supporting Information

ABSTRACT: Multilayers of poly(acrylic acid), PAA, and chitosan, CHI, have been built by the layer-by-layer (LbL) method from aqueous solutions at different pH values and analyzed by the dissipative quartz crystal microbalance (D-QCM) and ellipsometry. The results showed that under all of the assembly conditions considered the growth of the films is nonlinear. The thickness of the PAA layers increases as the pH of the assembling solutions decreases, whereas the adsorption of CHI is almost unaffected by the pH conditions. The comparison of the thickness obtained by D-QCM and by ellipsometry has allowed us to calculate the water content of the films, showing that the multilayers are highly hydrated, with an average water content higher than 20%. The analysis of D-QCM data has provided high-frequency values of the complex shear modulus that are in the megapascal range and shows a transition from mainly viscous to mainly elastic behavior for the added PAA layers, depending on the pH. The monomer surface density in each layer (obtained from the combination of ellipsometry and differential refractive index measurements) indicated that the monomer density depends on the assembly conditions. It was found that the adsorption kinetics is a bimodal process, with characteristic times that depend on the number and nature of the layers. Finally, the possibility of using of these multilayers as a drug storage and delivery system has been evaluated.



1. INTRODUCTION

During the last 20 years,^{1,2} polymer multilayers built by the layer-by-layer (LbL) technique have been frequently used in the fabrication of nanostructured coatings, being a cost-effective technique that allows us to produce materials that contain active compounds within their structure.^{3–5} One important advantage over classical techniques, such as the Langmuir–Blodgett (LB) technique,⁶ is the possibility of coating substrates with different chemical natures and shape such as colloidal particles,^{7,8} fluid interfaces,⁹ and liposomes,¹⁰ not being limited to flat solid substrates as more classical methods. In addition, the thermal stability of the films built by the LbL method is usually higher than that of the LB films.

In the last few years, many studies have been devoted to multilayers of synthetic polyelectrolytes. Some examples of these systems are multilayers of type (PDADMAC + PSS)_n

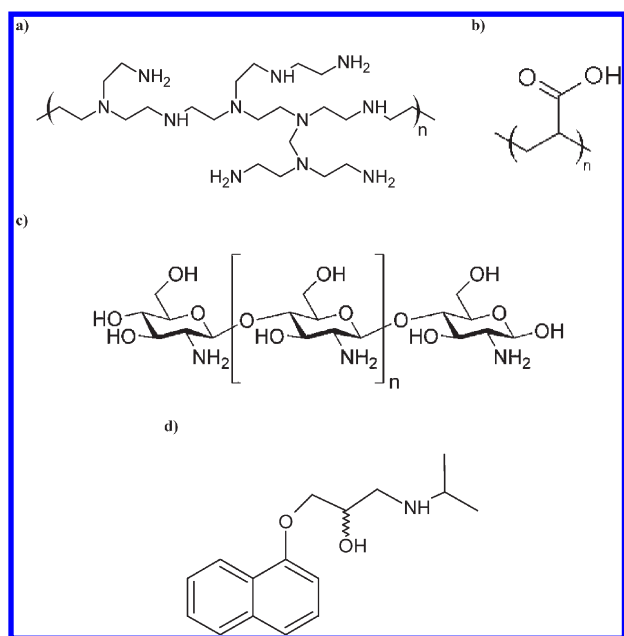
(PDADMAC is poly(diallyl-dimethyl-ammonium chloride) and PSS is poly(4-styrene sulfonate of sodium))^{11–13} or (PAH + PSS)_n (PAH is poly(allylamine hydrochloride)).¹⁴ However, nowadays there is increasing interest in building multilayers using biocompatible polymers,¹⁵ some examples of which are multilayers of type (PLL + HA)_n (PLL is poly(L-lysine) and HA is hyaluronic acid) or (PLL + PGA)_n (PGA is poly(glutamic acid)).^{16,17} The interest in this type of system is related to their applications in the biomedical field and for the fabrication of nanocapsules as drug delivery systems and in DNA encapsulation.^{2,18–20} Furthermore, the introduction of liposomes within multilayers is also a very active field of research,^{21,22} so they

Received: February 9, 2011

Revised: April 25, 2011

Published: May 11, 2011

Scheme 1. Chemical Structures of the Polymers Used in the Study^a



^a (a) PEI, (b) PAA, (c) CHI, and (d) propranolol.

can act as delivery agents or as microrreactors.^{23,24} More recently, some research groups have focused on the fabrication of biomimetic systems with multiscale organization. In these systems, different compartments are made by polyelectrolyte multilayers, and afterwards they are subsumed under a superior organizational unit also obtained by the LbL technique.^{25,26} However, to make coatings with controlled structures and physicochemical properties, it is necessary to know how different variables affect the building process. Some of these variables are the charge density of the polymers,^{27,28} polymer concentration,²⁹ ionic strength,^{12,30} solvent quality of the polyelectrolytes,¹¹ pH,³¹ and temperature,³² with the pH being the most important control parameter in the building of multilayers with weak polyelectrolytes because it determines the charge density of the chains.³³

The unique physicochemical (polycationic, reactive OH— and —NH₂ groups) and biological properties (bioactive, biocompatible, biodegradable, and nontoxic) have led to several research groups exploring the use of chitosan (CHI) in applications such as wastewater treatment,³⁴ cell growth support,³⁵ topical wound bandages,³⁵ and drug delivery systems.³⁶ Chitosan is an abundant amino-polysaccharide obtained from chitin (that is part of shrimp and crab shells) via deacetylation.^{35,37} It is a linear copolymer of 2-amino-2-deoxy-D-glucopyranose and 2-acetamide-2-deoxy-D-glycopyranose connected by glycosidic bonds $\beta(1 \rightarrow 4)$ (Scheme 1). The percentage of deacetylation is important to chitosan behavior because it determines its charge density and therefore its solubility and solution behavior³⁷ as well as its adsorption onto charged surfaces and the mechanical properties of the LbL multilayers. CHI has very good adhesion properties on skin, even under wet conditions (e.g., inside the mouth), which makes it a very good candidate for building storage/delivery multilayers for topical treatments.

The versatility of the LbL method allows us to build films with different shapes and geometries (nanoparticles, microspheres,

membranes, sponges, or rods).³⁸ Additionally, the physicochemical richness of the chitosan (tuning the charge density, biocompatibility, etc.) makes the multilayers with chitosan very attractive as drug carriers by different administration routes; in fact, several multilayers have already been studied: (CHI + alginate)_{*n*},³⁹ (CHI + PGA)_{*n*},⁴⁰ and (CHI + heparin)_{*n*}.⁴¹ In this work, we describe the building process, and the physicochemical properties of layer by layer multilayers formed by the combination of a natural polycation such as chitosan and a synthetic polyanion such as poly(acrylic acid) (PAA). The pH conditions chosen are imposed by the polyelectrolytes chosen. In effect, CHI and PAA precipitate at low pH values (and hydrolyze below pH 2), whereas at high pH values CHI is no longer charged. The pairs of pH values used to build the LbL multilayers were chosen to explore the limits of the pH ranges suitable for building multilayers of CHI and PAA and to include conditions in which the LbL multilayers might be used as drug delivery systems for topical treatments. The potential ability of these multilayers in drug delivery has been evaluated quantitatively by adsorbing propranolol (a beta-blocker drug that it is generally used for the treatment of hypertension problems) within the structure of the multilayers and analyzing the release process.

The results of the present work point out a strong effect of pH on the growing thickness of the multilayers. Also, it has been found for the first time that pH triggers a crossover from mainly viscous to mainly elastic behavior of the multilayers. Finally, the adsorbed amount of propranolol per polyelectrolyte bilayer has been found to increase with the number of bilayers, which is important for drug delivery purposes.

2. EXPERIMENTAL SECTION

2.1. Materials. The polyanion used was PAA ($pK_a \approx 4.8$) with a molecular weight of 450 kDa (purity higher than 99.5%). The polycation used was CHI (purity higher than 99.5%), purchased from Sigma-Aldrich (Germany) (with a degree of acetylation of 75–85%, $pK_a = 6.5$). Because of its natural origin, the CHI sample is polydisperse (molecular weight, M_w , of 50–190 kDa). The GPC study of CHI shows that there is only a broad molecular weight distribution and that the content of chains with a molecular weight lower than 50 kDa is negligible. However, it has already been pointed out that for $M_w > 10$ kDa the effect of M_w on the properties of the LbL multilayers is negligible.⁴² The first layer of highly branched poly(ethylene-imine) (PEI) of molecular weight 275 kDa (purity higher than 99.5%) was adsorbed onto the solid surface (for the molecular structure of the different polymers, see Scheme 1). The propranolol ((*R*)-(+)-propranolol hydrochloride) was purchased from Sigma-Aldrich (Germany). The pH of CHI and PAA solutions was controlled with glacial acetic acid (Sigma-Aldrich, purity >99.99%), HCl (Sigma-Aldrich, purity ~32%), and NaOH (Sigma-Aldrich, Germany); the pH of the PEI solutions was not adjusted. The water was of Milli-Q quality (Millipore RG model) with a resistivity higher than 18.2 M Ω and a total organic content lower than 10 ppb. All of the experiments were carried out at 298.1 \pm 0.1 K. The solutions were prepared by weight using an analytical balance with a precision of ± 0.01 mg. The multilayers that were studied are summarized in Table 1.

2.2. Experimental Techniques. A dissipative quartz-crystal microbalance (D-QCM) from KSV (model QCM Z-500, Finland) was used. The quartz crystals, AT-cut, were cleaned with piranha solution (70% H₂SO₄/30% H₂O₂) over a period of 30 min and then thoroughly rinsed with pure water. The characteristic frequency of the quartz crystal in vacuum was $f_0 \approx 5$ MHz. A self-assembled monolayer of the sodium salt of 3-mercapto propanesulfonic acid was initially built on the surface of the gold electrode of the quartz crystal in order to obtain a

Table 1. Resume of the Studied Samples^a

sample	pH _{PAA}	pH _{CHI}	nomenclature
multilayer 1	2.7	5	PEI (PAA _{pH 2.7} + CHI _{pH 5}) _{3,5}
multilayer 2	5	5	PEI (PAA _{pH 5} + CHI _{pH 5}) ₁₀
multilayer 3	7	6.5	PEI (PAA _{pH 7} + CHI _{pH 6.5}) ₁₀
multilayer 4	7	5	PEI (PAA _{pH 7} + CHI _{pH 5}) _{3,5}

^a Notice that the pK_a's are for PAA 4.8 and CHI 6.5. The subindex pH refers to the pH conditions of the solutions that are used.

charged substrate.¹² D-QCM provided the impedance spectra of the crystal for the fundamental resonance frequency and for its odd overtones, ν , up to the 11th (central frequency $f_{11} = 55$ MHz). The data have been analyzed using the model proposed by Johannsmann et al.⁴³ (further details are given in the Supporting Information). The injection of the solution into the QCM of a measuring cell leads to a dead time of 7 s; the data for shorter times were not taken into account for the data analysis.

For the ellipsometric experiments, we have used an imaging null ellipsometer from Nanofilm (model EP3, Germany), and all of the experiments have been carried out on a solid–liquid cell at a fixed angle of 60°. Silicon wafers (Siltronix, France) were used as the substrates.¹² Ellipsometric angles Δ and Ψ describe the changes in the state of polarization when light is reflected at a surface (further details given in the Supporting Information).⁴⁴ The uncertainty in Δ and Ψ were ± 0.1 and $\pm 0.05^\circ$, respectively. To obtain the ellipsometric thickness, h_{opt} , a four-layer model has been used, as in previous work.^{12,45} For the calculation of the adsorbed polymer mass (details given in the Supporting Information), the refractive index increment was measured with a Brookhaven differential refractometer (model BI-DNDC, USA).⁴⁶ The precision of $(dn/dc)_T$ was ± 0.001 mL/g. The values of $(dn/dc)_T$ for the different polymers used in this work are collected in Supporting Information (Table S.I). Shatz et al.⁴⁷ have shown that the influence of pH on the $(dn/dc)_T$ of solutions of CHI with a high degree of deacetylation is negligible. We have found the same for PAA solutions within the pH range used in this work.

The existence of charge overcompensation during the building process was evaluated by measuring the ζ potential (Zeta Nanosizer, Malvern Instruments, USA) of the bare silica particles (Sigma-Aldrich, Germany, 1 μm diameter), and we obtained $\zeta = -43$ mV in a water suspension of pH 5.6. The ionic strength of the measurements corresponded to the H⁺ concentration necessary to obtain pH 5.6. For the fabrication of the multilayers on silica particles, we have followed the method proposed by Sukhorukov et al.⁸ For each of the polyelectrolytes adsorbed, the ionic strength was given by H⁺ and the counterions.

Measurements of the contact angle, Θ , of a water drop on the surface of the multilayer were made using a commercial device from GBX (Model Digidrop, France). The precision of the measurements was obtained statistically from the results of the measurements in different zones of the samples.

2.3. Layer-by-Layer Assembly. The multilayers were built from polyelectrolyte solutions of concentration $c = 2$ mg \cdot mL⁻¹, except for the case of the layers of PEI (first layer in all of the multilayers studied) that were adsorbed from solutions of concentration $c = 1$ mg \cdot mL⁻¹. The even layers were made of PAA, and the odd layers were made of CHI. The adsorption of the layers was studied until equilibrium was detected by monitoring the changes in the frequency, Δf , and in the dissipation factor, ΔD , for the different overtones of the quartz crystal (with ν being the order of the overtone) as well as of the ellipsometric angles, Δ and Ψ . After the adsorption of each of the layers, the multilayers were rinsed with pure water. The rinsing process removed the polymer chains that were not strongly adsorbed but did not significantly modify the behavior of the multilayers (Supporting Information, Figure S.1). All of the

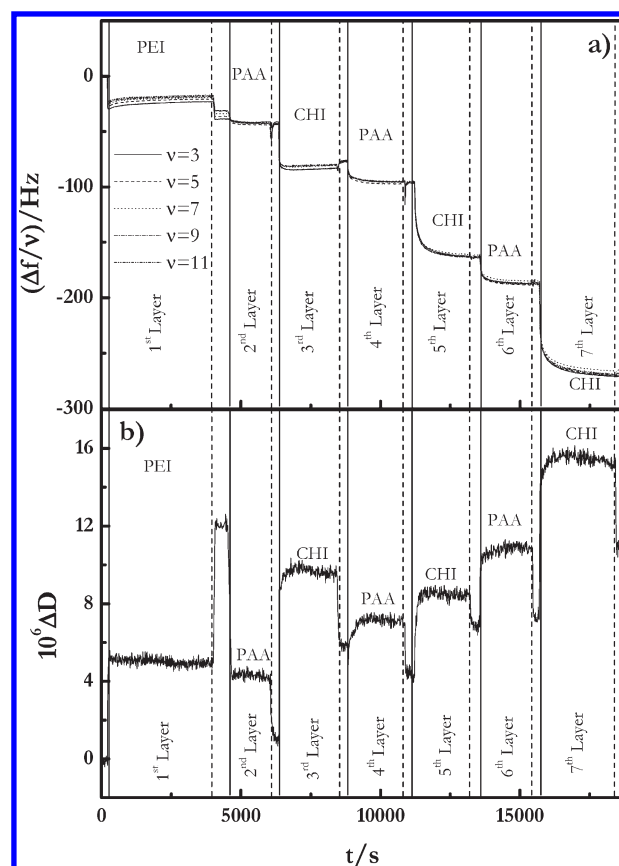


Figure 1. Dissipative quartz crystal microbalance results for the kinetics of adsorption and the washing-out process for the first seven layers of a PEI(PAA + CHI)_n multilayer, where PAA and CHI layers were assembled from solutions at pH 5. (a) Time dependence of the normalized frequency shifts for different overtones of the quartz sensor, $\Delta f/\nu$, with $\nu = 3, 5, 7, 9,$ and 11 being the overtone order. $\nu = 3$ (—), $\nu = 5$ (---), $\nu = 7$ (···), $\nu = 9$ (— · —), and $\nu = 11$ (— · · —) are shown. (b) Time dependence of the shift in the dissipation factor of the third overtone, ΔD . In both graphs, the vertical continuous lines (—) mark the polyelectrolyte injection, and the dashed lines (---) mark the washing with solvent.

experiments were performed under static conditions, without any stirring in the adsorption cell. The filling process of the measurement chamber took 10 s and sometimes led to an abrupt shift of the signal both in the D-QCM and in the ellipsometry techniques; these fast variations were discarded for the analysis of the adsorption process.⁴⁸ Propranolol layers were adsorbed from a water solution of concentration $c = 0.05$ mg \cdot mL⁻¹ after each CHI layer, being evaluated for the adsorbed amount of propranolol on different CHI layers. The kinetics of propranolol release for multilayers with 17 layers was measured by the D-QCM technique.

3. RESULTS

3.1. Multilayer Growth Process. Figure 1 shows the changes in the central frequency, f , for the different overtones (Figure 1a) and the dissipation factor for the third overtone (Figure 1b) during the adsorption of the first seven layers of a multilayer PEI(PAA_{pH 5} + CHI_{pH 5})_n. Similar trends were found for other multilayers assembled at the different combinations of pH studied. In addition to the expected decrease in f as the polymer chains adsorbed onto the quartz sensor, the rinsing process leads

to a small f shift. This shift is related to the reorganization of polymer chains within the film either as a consequence of the loss of some weakly bound chains or due to the swelling/deswelling processes of the adsorbed layers. In any case, it must be stressed that for all of the films studied in this work the frequency changes during the rinsing process were much smaller than those found during adsorption. This is in agreement with previously reported results that indicate that the adsorption of polyelectrolyte onto oppositely charged surfaces essentially leads to irreversible adsorbed layers.^{12,28,48}

The overtone dependence of the frequency shift is related to the mechanical properties of the films.⁴³ For purely elastic films (where the Sauerbrey equation applies), $\Delta f/\nu$ for all of the overtones should collapse onto a single master curve. However, as can be observed in Figure 1, the results show a small dependence of $\Delta f/\nu$ on the overtone number, which indicates that the film is viscoelastic and therefore the Sauerbrey equation (eq S.2) is not appropriated. This observation is confirmed by the behavior of the dissipation factor, D , (Figure 1b) that increases with the number of layers. Under these conditions, it is necessary to fit the full experimental impedance spectra to the theoretical predictions.⁴³ The spectra corresponding to $\nu = 3, 5, 7, 9,$ and 11 have been measured, which allows us to calculate the adsorbed mass and the real and imaginary components of the complex shear modulus, $\hat{G} = 1/\hat{J}$, of the polymer layer. (\hat{G} was assumed to be frequency-independent in the 15–55 MHz range⁴⁹). During the rinsing process of the CHI and PAA layers, we found a decrease in ΔD that may be explained as a consequence of the complexation process that leads to the entanglement between adjacent layers. In the case of the first layer, PEI, the behavior during the rinsing process is the inverse, probably resulting from the swelling of the highly branched PEI layer. The results obtained by ellipsometry are in qualitative agreement with D-QCM experiments (Supporting Information, Figure S.2).

3.2. Optical, h_{op} , and Acoustic, h_{ac} , Thicknesses. Figure 2a shows the shifts of the reduced frequency and the dissipation versus the number of layers, N , for PEI(PAA + CHI) $_n$ multilayers built under different pH combinations. The frequency shifts (Figure 2a) versus N show a nonlinear trend that is independent of the pH of the solutions, although for the multilayers with the smaller value of $-\Delta f/\nu$ this nonlinear trend is less evident and can be considered almost linear. However, the behavior of the different overtones (Figure 2a) depends on the assembly conditions: for all the multilayers, the different overtones collapse onto a master curve, $-\Delta f/\nu$ versus N , only for a small number of layers, which indicates that the films are rigid (Sauerbrey's limit). This separation between the curves of the different overtones takes place for lower values of N for the multilayers that have a faster growth rate, in agreement with the increase in the dissipation factor shown in Figure 2b.⁵⁰ The results obtained by ellipsometry are in qualitative agreement with the D-QCM results.

The analysis of the D-QCM data in terms of eq S.1 and the ellipsometry data in terms of the four-layer model led to the acoustical, h_{ac} and the optical, h_{op} , thicknesses shown in Figure 3. In all cases, $h_{ac} > h_{op}$ due to the fact that D-QCM detects both the adsorbed polymer and the water molecules coupled to it, whereas ellipsometry measures the amount of polymer adsorbed as a result of the fact that the refractive index of the polymer + water adsorbed layer is very similar to that of the polyelectrolyte solution.⁴⁶

3.3. Adsorption Kinetics. The adsorption kinetics of the layers has been found to be a bimodal process,^{51,52} in accordance with

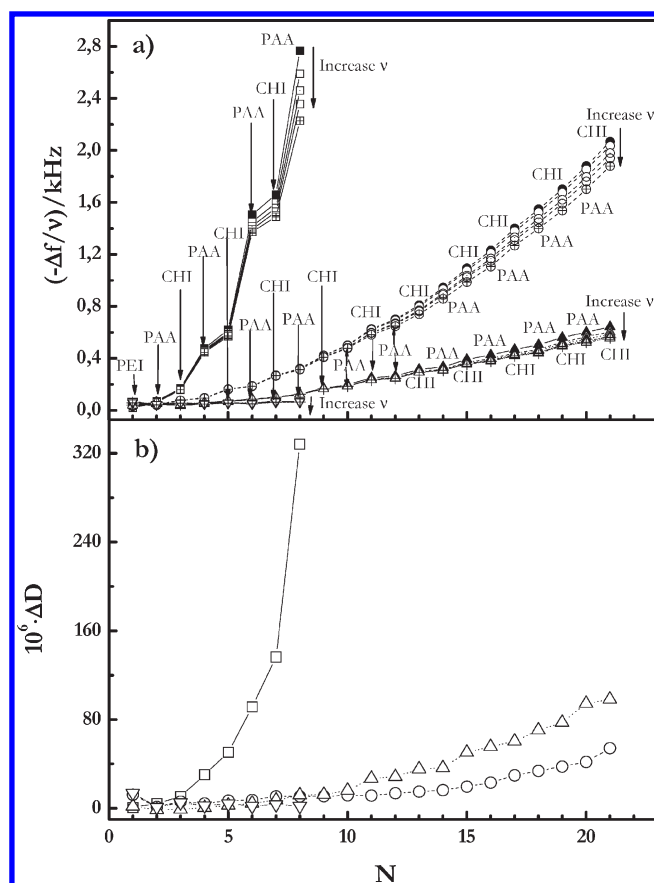


Figure 2. Multilayers PEI(PAA + CHI) $_n$ built using different pH combinations for the assembly of layers of PAA and CHI. (a) Number of layers' dependence of the reduced frequency of the quartz crystal for the different overtones measured (overtones $\nu = 3, 5, 7, 9,$ and 11 are shown for each experiment and are represented by different symbols). Notice that for low N the data for the different overtones collapse onto a single curve (rigid films) whereas at high N the data of the different overtones lie on different curves (viscoelastic film). All of the overtones for the same multilayer are represented with symbols of the same shape but different fill patterns: \blacksquare PEI(PAA $_{\text{pH } 2.7}$ + CHI $_{\text{pH } 5}$) $_n$, \bullet PEI(PAA $_{\text{pH } 5}$ + CHI $_{\text{pH } 5}$) $_n$, \blacktriangle PEI(PAA $_{\text{pH } 7}$ + CHI $_{\text{pH } 6.5}$) $_n$ and \blacktriangledown PEI(PAA $_{\text{pH } 7}$ + CHI $_{\text{pH } 5}$) $_n$. The arrows indicate the increase in the overtone order, ν . (b) Number of layers' dependence of the dissipation factor for the third overtone of the quartz crystal. Notice that the increase in the dissipation factor is stronger when the frequency shift is higher, which is in accordance with the behavior observed in the frequency shift of the different overtones. Legend: \square PEI(PAA $_{\text{pH } 2.7}$ + CHI $_{\text{pH } 5}$) $_n$, \circ PEI(PAA $_{\text{pH } 5}$ + CHI $_{\text{pH } 5}$) $_n$, \triangle PEI(PAA $_{\text{pH } 7}$ + CHI $_{\text{pH } 6.5}$) $_n$ and ∇ PEI(PAA $_{\text{pH } 7}$ + CHI $_{\text{pH } 5}$) $_n$.

the results previously reported for other multilayers.^{12,48,53,54} The first process is a fast adsorption step probably related to the transport of chains to the surface, accompanied by fast mass deposition; however, it is not diffusion-controlled because the adsorbed mass does not show a $t^{1/2}$ dependence. This is in agreement with the mean-field calculation results for the study of the adsorption process of polyelectrolyte by Cohen-Stuart et al.⁵⁵ The second and slower process may be related to the internal reorganization of the polymer chains in the multilayer.^{53,56} In recent work, Lane et al.⁵⁶ studied the adsorption kinetics of multilayers of PSS and poly[1-[4[(3-carboxy-4-hydroxyphenylazo)-benzenesulfonamido]-1,2-ethanediyl sodium salt] using dual-beam polarization interferometry and D-QCM, and they explained the

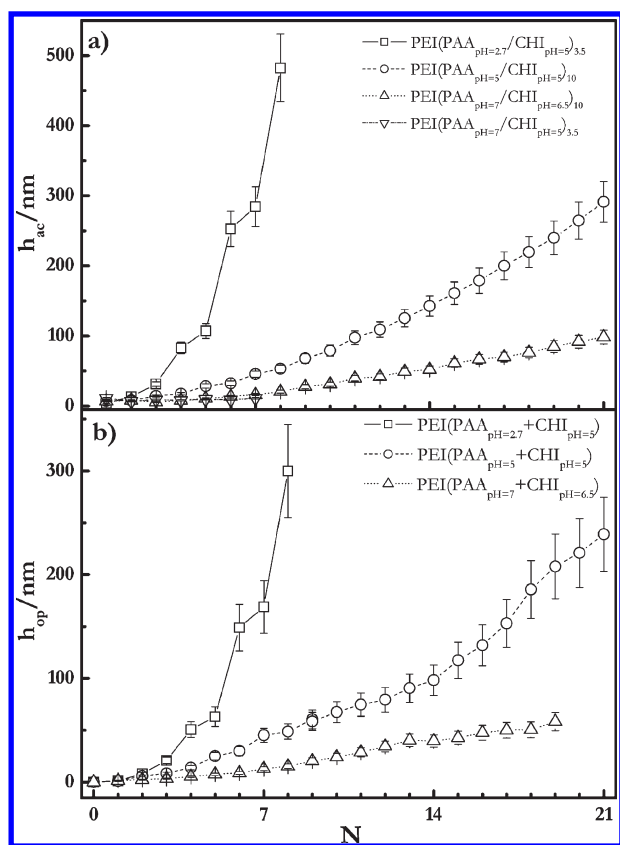


Figure 3. Thickness obtained using D-QCM and ellipsometry for multilayers PEI(PAA + CHI)_n built using different pH combinations for the assembly of layers of PAA and CHI. (a) D-QCM and (b) ellipsometric results.

adsorption kinetics in terms of three different processes, which is in accordance with the Brownian dynamics simulations of Linse and Källrot for neutral polymers.⁵⁷ However, our experimental results seem to be in accordance with the mean-field calculations by Cohen-Stuart et al.⁵⁵ and can be described by the model proposed by Raposo et al.⁵³ (more details are given in the Supporting Information; see Figure S.3). Equation S.9 describes the experimental data within experimental precision independently of the polyelectrolyte type and the layer number. This behavior was observed previously for multilayers of (PDADMAC + PSS)_n.^{12,48}

Figure 4 shows the characteristic times of adsorption for both processes in the different multilayers studied. In all cases, τ_2 is almost 1 order of magnitude larger than τ_1 . (It must be stressed that τ_1 is well above the dead time of the experimental techniques used in this work.) The two characteristic times, τ_1 and τ_2 , depend on the number of layers of PAA, whereas for CHI only τ_2 depends on the layer number.

4. DISCUSSION

The results presented above clearly point out that the growth and properties of the multilayers studied present a strong dependence on the pH of the polyelectrolyte solutions used for the assembly of the different layers. This may be understood by considering the changes in the charge density of the polymer chains with pH, thus modifying the interactions between polyelectrolytes in the building process.

4.1. Adsorption Kinetics. In PEI(PAA_{pH_x} + CHI_{pH_y})_n multilayers, the two characteristic times, τ_1 and τ_2 , increase with the layer number for the adsorption of PAA layers. However, the behavior for the adsorption of CHI layers is slightly different, and only the reorganization time τ_2 depends on the number of layers.⁵⁸ These dependences may be explained as a result of the in and out interdiffusion of polymer chains through the LbL multilayer during the adsorption process of both polymers.¹⁶ As a consequence, the kinetics of the adsorption of the different layers depends on the layer adsorbed previously,^{48,59} in agreement with the model proposed by Lavalle et al. for nonlinear growth.⁶⁰

In the case of CHI layers, the adsorption times do not depend on the pH because of the rigidity of the CHI chains.⁶¹ However, for the PAA layers, τ_1 and τ_2 depend on the pH conditions used for the assembly (Figure 4a,c): As the pH increases, both characteristic times decrease and show a smaller dependence on the number of layers. This behavior may be understood by considering that at lower pH the LbL multilayers grow in a more nonlinear way and the interdiffusion of the chains during the assembly is more important, in agreement with the results recently reported by Bieker and Schönhoff for multilayers PEI-(PAA + PAH)_n.³³ In addition, the decrease in the pH leads to a lower charge density in the PAA chains, thus making the interaction with the charged surface less favorable and slowing down the adsorption process.⁶⁰

4.2. Multilayer Growth. To understand the growth of the PEI(PAA_{pH_x} + CHI_{pH_y})_n multilayers, one must recall that PAA and CHI are weak polyelectrolytes.³³ Shiratori et al. have reported that the thickness of the PAA layers strongly depends on the pH.⁶² However, the effect of the pH on the adsorption of the layers of CHI is almost negligible under the conditions used in this work because the rigidity of the chains reduces the effect of the pH on the conformation of the chains. As a consequence, the changes observed in the thickness of the layers are mostly due to the effect of pH on the PAA chains.

Notice that for pH 2.7 the thickness increase of the PAA layers seems to be higher than that expected for a single polymer monolayer (Figure 3).¹² It is known that an important driving force in the nonlinear growth of polyelectrolyte multilayers is the in and out diffusion of the polymer chains through the multilayers^{17,60} that is related to the Donnan equilibrium within the multilayer.⁶³ When a PAA layer is adsorbed at pH 2.7, the CHI layer onto which PAA adsorbs increases its charge density, which, because of the Donnan equilibrium, facilitates the in and out diffusion of the PAA chains until charge inversion is attained. This enhanced diffusion process leads to an increase in the amount of PAA adsorbed.⁶⁰

As mentioned above, multilayers with slower growth (higher pH of the PAA solutions) present an almost linear variation of the thickness with the number of layers. Under these conditions, the charge density of the PAA chains is higher, thus decreasing the diffusion through the multilayer. Furthermore, the increase in the charge density of adsorbed CHI chains is smaller for the higher pH used because the increase of pH inhibits the interdiffusion of PAA through the multilayer structure. These results agree with those reported by Richert et al. for (CHI + HA)_n multilayers⁶⁴ and by Bieker and Schönhoff for PEI(PAA + PAH)_n multilayers.³³ In the case of the adsorption of CHI layers, it is not possible to rule out the contribution of the in and out interdiffusion on the adsorption of the layers.⁵⁸ In this case, the different conditions used for the assembly of CHI layers

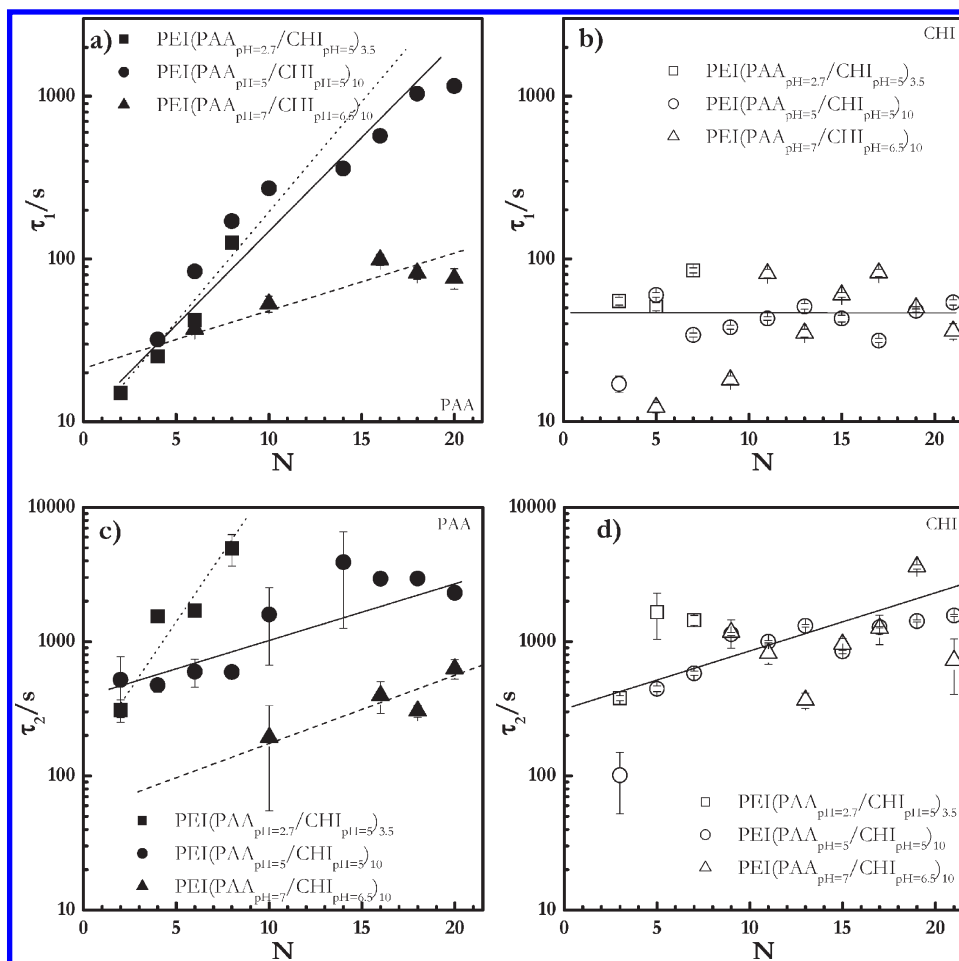


Figure 4. Times for the adsorption of the layers of PAA and CHI in two different PEI(PAA + CHI)_n multilayers (a) τ_1 for PAA: ■ PEI(PAA_{pH 2.7} + CHI_{pH 5})_n, ● PEI(PAA_{pH 5} + CHI_{pH 5})_n and ▲ PEI(PAA_{pH 7} + CHI_{pH 6.5})_n. (b) τ_1 for CHI: □ PEI(PAA_{pH 2.7} + CHI_{pH 5})_n, ○ PEI(PAA_{pH 5} + CHI_{pH 5})_n and △ PEI(PAA_{pH 7} + CHI_{pH 6.5})_n. (c) τ_2 for PAA: ■ PEI(PAA_{pH 2.7} + CHI_{pH 5})_n, ● PEI(PAA_{pH 5} + CHI_{pH 5})_n and ▲ PEI(PAA_{pH 7} + CHI_{pH 6.5})_n. (d) τ_2 for CHI: □ PEI(PAA_{pH 2.7} + CHI_{pH 5})_n, ○ PEI(PAA_{pH 5} + CHI_{pH 5})_n and △ PEI(PAA_{pH 7} + CHI_{pH 6.5})_n. The lines are guides for the eyes.

(pH 5 and 6.5) lead to a similar degree of ionization on the adsorbed PAA layers, as determined by Bieker and Schönhoff using ATR-FTIR.³³ This leads to a similar negatively charged structure for both pH conditions, thus producing a similar contribution of CHI interdiffusion.

4.3. Charge Compensation. It is well known that charge overcompensation is the driving force for the construction of multilayers by electrostatic self-assembly.^{65,66} Figure 5 shows the changes in the ζ potential measured after coating colloidal particles with multilayers of PEI(PAA_{pH x} + CHI_{pH y})_n with *N* layers. The adsorption of PEI directly onto the silica particles leads to a high overcompensation,⁶⁷ which decreases as the number of layers (CHI or PAA) increases for all assembly conditions. This may be due to the formation of layers that are a blend of CHI and PAA chains with a structure similar to that of the interpolyelectrolyte complex as observed by Svensson et al. in (CHI + mucin)_n multilayers.⁶⁸ This interpolyelectrolyte complexlike structure is stabilized by the effect of the entropy gain associated with the release of water molecules and the formation of hydrogen bonds between the backbone of the CHI chains and the PAA chains.¹⁶ Similar behavior was found for the contact angle measurements of water drops on the multilayers as already reported by Zembala et al.⁶⁹ for (PAH+PSS)_n multilayers (Figure S.4 in the Supporting Information).

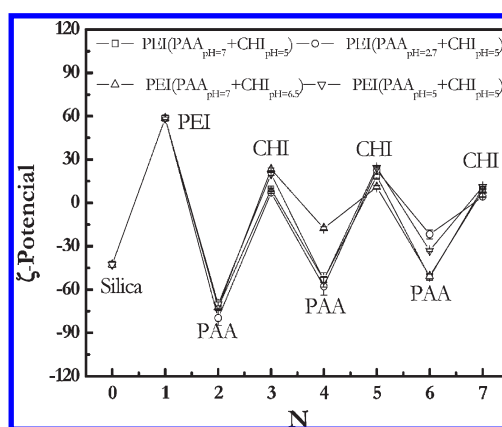


Figure 5. ζ potential for the different multilayers adsorbed on colloidal particles.

In spite of the overcompensation, the films have to be electrically neutral from a macroscopic point of view (at a length scale beyond the Debye length). During the adsorption process, the surface charge of the adsorbed polyelectrolytes must be neutralized either by monomers of the preceding polymer layer

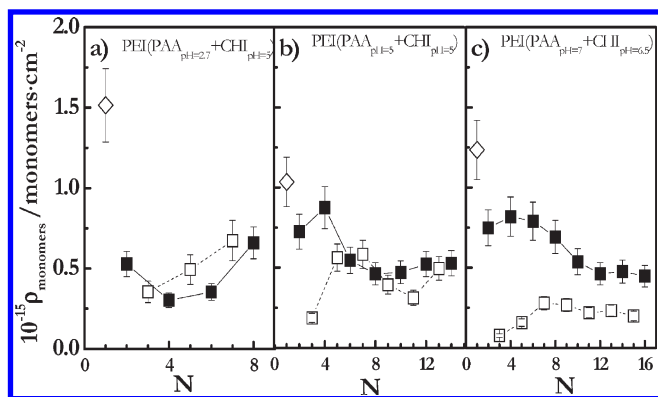


Figure 6. Surface concentration of ionizable adsorbed monomers in each cycle for multilayers PEI(PAA_{pH_x} + CHI_{pH_y})_n assembled under different conditions. (a) PEI(PAA_{pH=2.7} + CHI_{pH=5})_n, (b) PEI(PAA_{pH=5} + CHI_{pH=5})_n, (c) PEI(PAA_{pH=7} + CHI_{pH=6.5})_n. Legend (the same in all the cases): \diamond PEI, \blacksquare PAA, and \square CHI.

(intrinsic mechanism) or by counterions in the polymer solution (extrinsic mechanism). The existence of only intrinsic compensation implies a stoichiometric 1:1 ratio (polyanion monomer unit/polycation monomer unit) in the multilayer, whereas for extrinsic compensation other stoichiometries can be found. A simple way to evaluate the charge-compensation mechanism is to measure the number of monomer units of PAA adsorbed per ionizable monomer unit of the CHI chains adsorbed in the next layer. We have calculated the monomer unit surface density, $\rho_{monomer}$, of PEI, PAA, and CHI for each adsorption cycle (details in the Supporting Information).^{12,28,48,59} When the number of monomer units of adjacent layers is the same, the compensation is intrinsic; otherwise, the compensation mechanism is extrinsic. Notice that intrinsic compensation in the multilayer does not mean exact matching between the charged monomer units on layers of CHI and PAA but matching between the total number of ionizable monomer units in the multilayer. The ratio of the adsorbed monomer units of CHI and PAA in Figure 6 depends on the pH used for the assembly, and the results show that for low and high pH values of assembly for PAA the compensation mechanism may be considered to be intrinsic and extrinsic, respectively, during the whole building process. However, when both polyelectrolytes were assembled at pH 5 a transition between extrinsic compensation and intrinsic compensation was observed for $N = 4$.

4.4. Water Content. Polymer chains and counterions adsorb in a hydrated form. The water weight fraction associated with the multilayer, X_w , can be obtained by comparing the mass obtained by D-QCM and ellipsometry and using eq S.10;^{12,70–72} it was shown that this method gives values of X_w that are in good agreement with those provided by neutron reflectivity.¹² Figure 7 shows that X_w decreases from high values for a small number of layers to a quasi-plateau that depends on the assembly conditions although it is in the 0.2–0.4 range in all cases. These unexpected low values obtained for multilayers containing polysaccharides^{68,73} may be due to the interpenetrated character of the films that induces the expulsion of water out of the multilayer, stabilizing a highly entangled structure.^{12,16,73} These results agree with the results previously reported for multilayers of (PDADMAC + PSS)_n^{12,48} and (PAH + PSS)_n.⁷⁴ The qualitative behavior of X_w versus N is independent of the assembly conditions, which can be explained by the same

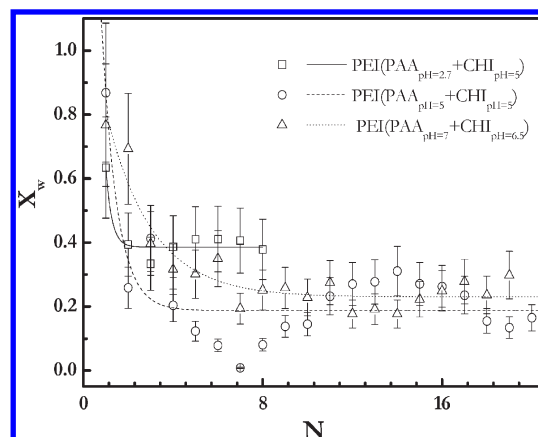


Figure 7. Water contents for different studied PEI(PAA_{pH_x} + CHI_{pH_y})_n multilayers. The points are the calculated data, and the lines are only guides for the eyes that show the average behavior of the results. In all of the multilayers, the first layer is always the PEI layer.

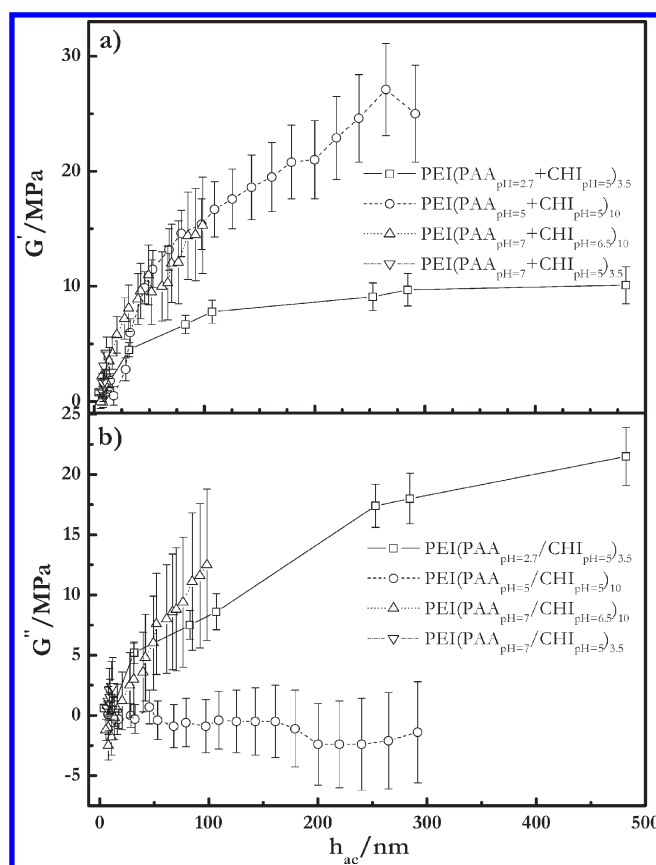


Figure 8. Mechanical properties. (a) G' vs h_{ac} . (b) G'' vs h_{ac} .

arguments used in the previous section to explain the ζ -potential results.^{16,75}

4.5. Mechanical Properties. The behavior of the real and imaginary parts of the shear modulus, G' and G'' , obtained from the analysis of the D-QCM experiments (eq S.1) is shown in Figure 8. In all of the multilayers studied, G' and G'' are in the MPa range, which corresponds to the rubbery region of typical polymers in the low-frequency range (below 100 Hz). This is reasonable considering that the multilayers are highly plasticized

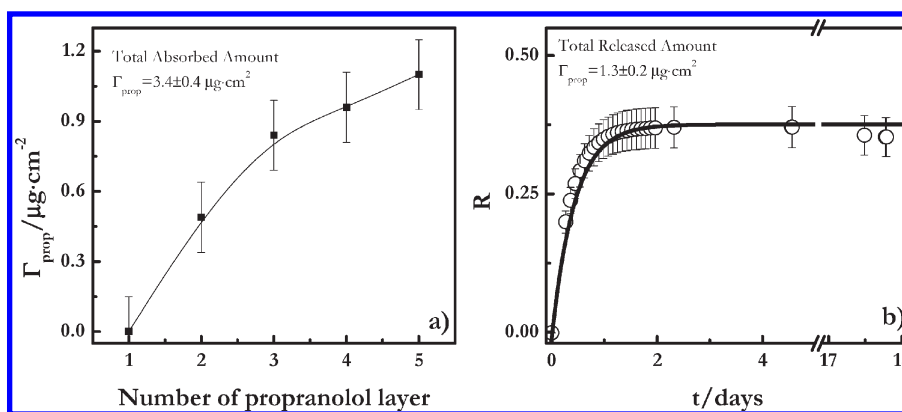


Figure 9. (a) Adsorbed amount of propranolol per layer, Γ_{prop} as a function of the number of propranolol layers adsorbed. (b) Releasing kinetics of propranolol from a multilayer with 5 layers of propranolol and 12 layers of polyelectrolyte. $R = 1 - [\Gamma_{\text{prop}}/\Gamma_{\text{prop}}(0)]$ is the relative amount of propranolol released from the multilayer. The symbols represent the experimental data, and the solid line is the fit to the first-order kinetics.

by water,⁷⁶ and it is in agreement with the results reported for other wet multilayers.^{12,28,48}

The behavior of the films in which the layers of PAA were assembled from low-pH solutions shows that they have an essentially viscous character with $G'' \gg G'$, which corresponds to diffuse structures that are able to dissipate energy. When the PAA layers are assembled from pH 5 solutions, the films behave as an elastic body. However, upon increasing the pH of the PAA solutions, the values of G' become close to those of G'' , thus suggesting that the multilayer behaves as a gel at the high frequencies of our measurements.⁷⁶ This is the first time that such a pH-induced crossover from mainly viscous to mainly elastic behavior has been reported, which might be useful in tuning the permeability of small molecules through the multilayer (e.g., in polyelectrolyte-coated nanocapsules). In general, the increase in X_w leads to soft layers with higher values of G'' ; the inverse behavior was found for multilayers with low values of X_w , where the elastic part of the shear modulus is higher (Figure S.7 in the Supporting Information).

4.6. Multilayers as Drug-Delivery Systems. Figure 9a shows the adsorbed amount of propranolol, Γ_{prop} , onto the different CHI layers assembled at pH 5. This drug was chosen because it is an efficient beta blocker that may interact with PAA and CHI via the formation of hydrogen bonds and/or electrostatic interactions. Drug storage and delivery from multilayers are important to topical treatments. The results show that the adsorbed amount of propranolol per layer increases with the number of layers, which may be due to the diffusion of propranolol molecules into the interior of the multilayer. The total adsorbed amount of propranolol for a multilayer with 22 layers (5 of them are propranolol) was $\Gamma_{\text{prop}}(0) = 3.4 \pm 0.4 \mu\text{g} \cdot \text{cm}^{-2}$.

Figure 9b shows the kinetics of releasing propranolol from a multilayer assembled at pH 5. The relative amount of propranolol released from the multilayer, $R = 1 - [\Gamma_{\text{prop}}/\Gamma_{\text{prop}}(0)]$ versus time may be modeled as first-order kinetics⁷⁶ with a characteristic time of $\tau_{\text{releasing}} = 0.43 \pm 0.3$ days (~ 10.3 h), which may be considered to be a relatively fast releasing process for topical pharmaceutical treatments. Notice that after 18 days the total amount of propranolol released is only $1.3 \pm 0.3 \mu\text{g} \cdot \text{cm}^{-2}$, which is less than half the total amount adsorbed. In fact, it is not possible to rule out that the amount released is only the one adsorbed in the last two layers of propranolol (the amount adsorbed in the last layer was $1.1 \pm 0.1 \mu\text{g} \cdot \text{cm}^{-2}$). This may be

due to the role of propranolol as a cross-linker of the polyelectrolyte matrix via hydrogen bonding. In spite of the fact that only 38% of the propranolol is released over a 2 day period, it has to be kept in mind that the use of multilayers may be useful because the amount of propranolol adsorbed in each layer increases with the number of layers in the film as a result of the nonlinear growth regime.

5. CONCLUSIONS

The electrostatic self-assembly of PAA and CHI has been studied by D-QCM and ellipsometry. The effect of the pH of the solutions on the assembly of the layers has been discussed. Both techniques indicated that the adsorption of both polyelectrolytes is essentially irreversible. The growth mechanism is nonlinear (exponential) independent of the pH used for the assembly, although for the multilayers that grow at a slower rate the growth looks linear. The surface density of monomers shows an excess of ionizable monomers that depends on the assembly conditions, with it being possible to control the mechanism of charge compensation by modifying the pH of the solutions of PAA and CHI. The comparison of the thickness values obtained from D-QCM and ellipsometry has allowed us to estimate the water content in the multilayers. In general, the overall water content decreases as the number of layers increases, being quite large for films with a small number of layers. For films with a large number of layers, the water content remains almost constant with N , the value of the plateau depending on the assembly conditions. The complex shear modulus of the film thickness was obtained from D-QCM, showing G' and G'' values in the range of a few MPas. It has been possible to modulate the mechanical properties for the assembly conditions of PAA, going from purely elastic films to quasi-purely viscous films. The mechanical properties of the films are strongly correlated with the water content of the multilayer. In all cases studied, it was found that the adsorption followed bimodal kinetics whose characteristic adsorption times depend on the number of layers for the different adsorbed layers. The adsorption times for both processes depend on the assembly conditions in the case of PAA layers; however, for the CHI layers, no dependence on the assembly conditions was found. This is probably related to the rigidity of the CHI chains, which can be tuned by changing the degree of deacetylation of the chitin precursor. The multilayers studied may act as drug storage and

delivery systems. Although the propranolol released is only 37% of the total amount adsorbed at pH 5, it has been found that the amount of propranolol adsorbed in each layer increases with the number of layers of the polymer film, which may be useful for drug delivery. The effect of pH on the values of G' and G'' can be used to tune the permeability of the LbL multilayers and therefore the kinetics of drug delivery.

■ ASSOCIATED CONTENT

S Supporting Information. Extended details of the experiments, models used in the present study, and auxiliary results. This material is available free of charge via the Internet at <http://pubs.acs.org>.

■ AUTHOR INFORMATION

Corresponding Author

*E-mail: mcs@fcq.unc.edu.ar; rgrubio@quim.ucm.es.

Present Addresses

[§]CNR-Istituto per L'Energetica e le Interfasi, Via De Marini 6, 16149-Genova, Italy

■ ACKNOWLEDGMENT

This work was supported in part by MICINN under grant FIS2009-14008-C02-01, by the ESA under grant MAP AO-00-052, and by the EU under the MULTIFLOW excellence network of the 7th FP. E.G. was supported by a FPU fellowship from MICINN. We are grateful to the UIRC of the CAI of Spectroscopy of Complutense University for the use of the ellipsometer.

■ REFERENCES

- (1) Decher, G. *Science* **1997**, *277*, 1232.
- (2) Decher, G.; Schlenoff, J. B. *Multilayer Thin Films: Sequential Assembly of Nanocomposite Materials*; Wiley-VCH: Berlin, 2003.
- (3) Schoeler, B.; Delorme, N.; Doench, I.; Shukhorukov, G. B.; Fery, A.; Glinel, K. *Biomacromolecules* **2006**, *7*, 2065.
- (4) Boulmedais, F.; Ball, V.; Schwinte, P.; Frisch, B.; Schaaf, P.; Voegel, J. C. *Langmuir* **2003**, *19*, 440.
- (5) Chluba, J.; Voegel, J.-C.; Decher, G.; Erbacher, P.; Schaaf, P.; Ogier, J. *Biomacromolecules* **2001**, *2*, 800.
- (6) Blodgett, K. B. *J. Am. Chem. Soc.* **1934**, *56*, 495.
- (7) Caruso, F.; Lichtenfeld, H.; Giersig, M.; Möhwald, H. *J. Am. Chem. Soc.* **1998**, *120*, 8523.
- (8) Sukhorukov, G. B.; Donath, E.; Davis, S.; Lichtenfeld, H.; Caruso, F.; Popov, V. I.; Möhwald, H. *Polym. Adv. Technol.* **1998**, *9*, 759.
- (9) Ferri, J. K.; Kotsmar, C.; Miller, R. *Adv. Colloid Interface Sci.* **2010**, *161*, 29.
- (10) Yaroslavov, A. A.; Rakhnyanskaya, A. A.; Yaroslavova, E. G.; Efimova, A. A.; Menger, F. M. *Adv. Colloid Interface Sci.* **2008**, *142*, 43.
- (11) Dubas, S. T.; Schlenoff, J. B. *Macromolecules* **1999**, *32*, 8153.
- (12) Guzmán, E.; Ritacco, H.; Rubio, J. E. F.; Rubio, R. G.; Ortega, F. *Soft Matter* **2009**, *5*, 2130.
- (13) Ramos, J. J. I.; Llarena, I.; Moya, S. E. *J. Mater. Sci.* **2010**, *48*, 4970.
- (14) Ladam, G.; Schaad, P.; Voegel, J. C.; Schaaf, P.; Decher, G.; Cuisinier, F. *Langmuir* **2000**, *16*, 1249.
- (15) Lee, K. Y.; Mooney, D. J. *Chem. Rev.* **2001**, *101*, 1869.
- (16) Picart, C.; Lavalle, P.; Hubert, P.; Cuisinier, F. J. G.; Decher, G.; Schaaf, P.; Voegel, J. C. *Langmuir* **2001**, *17*, 7414.
- (17) Picart, C.; Mutterer, J.; Richert, L.; Luo, Y.; Prestwich, G. D.; Schaaf, P.; Voegel, J. C.; Lavalle, P. *Proc. Nat. Acad. Sci. U.S.A.* **2002**, *99*, 12531.
- (18) Cheung, J. H.; Fou, A. F.; Rubner, M. F. *Thin Solid Films* **1994**, *244*, 985.
- (19) Shchukin, D. G.; Möhwald, H. *Small* **2007**, *3*, 926.
- (20) Antipov, A. A.; Sukhorukov, G. B.; Donath, E.; Möhwald, H. *J. Phys. Chem. B* **2001**, *105*, 2281.
- (21) Michel, M.; Izquierdo, A.; Decher, G.; Voegel, J.-C.; Schaaf, P.; Ball, V. *Langmuir* **2005**, *21*, 7854.
- (22) Michel, M.; Vautier, D.; Voegel, J. C.; Schaaf, P.; Ball, V. *Langmuir* **2004**, *20*, 4835.
- (23) Michel, M.; Arntz, Y.; Fleith, G.; Toquant, J.; Haikel, Y.; Voegel, J. C.; Schaaf, P.; Ball, V. *Langmuir* **2006**, *22*, 2358.
- (24) Malcher, M.; Volodkin, D.; Heurtault, B.; Andr, P.; Schaaf, P.; Möhwald, H.; Voegel, J.-C.; Sokolowski, A.; Ball, V.; Boulmedais, F.; Frisch, B. *Langmuir* **2008**, *24*, 10209.
- (25) Stadler, B.; Chandrawati, R.; Price, A. D.; Chong, S. F.; Breheny, K.; Postma, A.; Connal, L. A.; Zelikin, A. N.; Caruso, F. *Angew. Chem., Int. Ed.* **2009**, *48*, 4359.
- (26) Stadler, B.; Price, A. D.; Chandrawati, R.; Hosta-Rigau, L.; Zelikin, A. N.; Caruso, F. *Nanoscale* **2009**, *1*, 68.
- (27) Steitz, R.; Jaeger, W.; von Klitzing, R. *Langmuir* **2001**, *17*, 4471.
- (28) Guzmán, E.; San Miguel, V.; Peinado, C.; Ortega, F.; Rubio, R. G. *Langmuir* **2010**, *26*, 11494.
- (29) Saarinen, T.; Österberg, M.; Laine, J. *Colloids Surf., A* **2008**, *330*, 134.
- (30) Schlenoff, J. B.; Dubas, S. T. *Macromolecules* **2001**, *34*, 592.
- (31) Zhang, X.; Sun, Y. P.; Gag, M. L.; Kong, X. X.; Shen, J. C. *Macromol. Chem. Phys.* **1996**, *197*, 509.
- (32) Salomaki, M.; Vinokurov, I. A.; Kankare, J. *Langmuir* **2005**, *21*, 11232.
- (33) Bieker, P.; Schönhoff, M. *Macromolecules* **2010**, *43*, 5052.
- (34) Bhatnager, A.; Sillanpää, M. *Adv. Colloid Interface Sci.* **2009**, *152*, 26.
- (35) Khor, E. *Chitin: Fulfilling a Biomaterial Promise*; Elsevier: Amsterdam, The Netherlands, 2001.
- (36) Devanga-Chinta, D.; Graves, R. A.; Pamujula, S.; Mandal, T. K. *Drug Dev. Ind. Pharm.* **2010**, *36*, 200.
- (37) Muzzarelli, R. A. A. *Natural Chelating Polymers: Alginic Acids, Chitin, and Chitosan*; Pergamon Press: Oxford, U.K., 1973.
- (38) Denkbass, E. B. *J. Bioact. Compat. Polym.* **2006**, *21*, 351.
- (39) Yuan, W.; Dong, H.; Li, C. M.; Cui, X.; Yu, L.; Lud, Z.; Zhou, Q. *Langmuir* **2007**, *23*, 13046.
- (40) Song, Z.; Yin, J.; Luo, K.; Zheng, Y.; Yang, Y.; Li, Q.; Yan, S.; Chen, X. *Macromol. Biosci.* **2009**, *9*, 268.
- (41) Boddohi, S.; Killingsworth, C. E.; Kipper, M. J. *Biomacromolecules* **2008**, *9*, 2021.
- (42) Zui, Z.; Salloum, D.; Schlenoff, J. B. *Langmuir* **2003**, *19*, 2491.
- (43) Johannsmann, D.; Mathauer, K.; Wegner, G.; Knoll, W. *Phys. Rev. B* **1992**, *46*, 7808.
- (44) Azzam, R. M. A.; Bashara, N. M. *Ellipsometry and Polarized Light*; Elsevier: North-Holland, 1987.
- (45) Tompkins, H. G. *A User's Guide to Ellipsometry*; Academic Press: Amsterdam, 1993.
- (46) Höök, F.; Kasemo, B.; Nylander, T.; Fant, C.; Scott, K.; Elwing, H. *Anal. Chem.* **2001**, *73*, 5796.
- (47) Schatz, C.; Pichot, C.; Delair, T.; Viton, C.; Domard, A. *Langmuir* **2003**, *19*, 9896.
- (48) Guzmán, E.; Ritacco, H.; Ortega, F.; Svitova, T.; Radke, C. J.; Rubio, R. G. *J. Phys. Chem. B* **2009**, *113*, 7128.
- (49) Steinem, C.; Janshoff, A. Specific Adsorption of Annexin A1 on Solid-Supported Membranes: A Model Study. In *Piezoelectric Sensors; Wolfbeis, O. S., Steinem, C., Janshoff, A., Eds.; Springer Series on Chemical Sensors and Biosensors; Springer-Verlag: Berlin, 2007*, p 281.
- (50) Salomaki, M.; Kankare, J. *J. Phys. Chem. B* **2007**, *111*, 8509.
- (51) Chiang, C.-Y.; Starov, V. M.; Hall, M. S.; Lloyd, D. R. *Colloid J.* **1997**, *59*, 236.
- (52) Chiang, C.-Y.; Starov, V. M.; Lloyd, D. R. *Colloid J.* **1995**, *57*, 715.
- (53) Raposo, M.; Pontes, R. S.; Mattoso, L. H. C.; Oliveira, O. N. *Macromolecules* **1997**, *30*, 6095.

- (54) Guzmán, E.; Ortega, F.; Baghdadli, N.; Luengo, G. S.; Rubio, R. G. *Colloids Surf, A* **2011**, *375*, 209.
- (55) Cohen-Stuart, M. A. *J. Phys. (Paris)* **1997**, *9*, 7767.
- (56) Lane, T. J.; Fletcher, W. R.; Gormally, M. V.; Johal, M. S. *Langmuir* **2008**, *24*, 10633.
- (57) Linse, P.; Källrot, N. *Macromolecules* **2010**, *43*, 2054.
- (58) Lundin, M.; Blomberg, E.; Tilton, R. D. *Langmuir* **2010**, *26*, 3242.
- (59) Guzmán, E.; Ortega, F.; Prolongo, M. G.; Rubio, M. A.; Rubio, R. G. *J. Mater. Sci. Eng.* **2010**, *4*, 1.
- (60) Lavalle, P.; Picart, C.; Mutterer, J.; Gergely, C.; Reiss, H.; Voegel, J. C.; Senger, B.; Schaaf, P. *J. Phys. Chem. B* **2004**, *108*, 635.
- (61) Kleinschmidt, F.; Stutbenrauch, C.; Delacotte, J.; von Klitzing, R.; Langevin, D. *J. Phys. Chem. B* **2009**, *113*, 3972.
- (62) Shiratori, S. S.; Rubner, M. F. *Macromolecules* **2000**, *33*, 4213.
- (63) Laugel, N.; Boulmedais, F.; Haitami, A. E. E.; Rabu, P.; Rogez, G.; Voegel, J.-C.; Schaaf, P.; Ball, V. *Langmuir* **2009**, *25*, 14030.
- (64) Richert, L.; Lavalle, P.; Payan, E.; Shu, X. Z.; Prestwich, G. D.; J.-F., S.; Schaaf, P.; Voegel, J.-C.; Picart, C. *Langmuir* **2004**, *20*, 448.
- (65) Caruso, F.; Donath, E.; Möhwald, H. *J. Phys. Chem. B* **1998**, *102*, 2011.
- (66) Grosberg, A. Y.; Nguyen, T. T.; Shklovskii, B. I. *Rev. Mod. Phys.* **2002**, *74*, 329.
- (67) Gorin, D. A.; Yashchenok, A. M.; Manturov, A. O.; Kolesnikova, T. A.; Möhwald, H. *Langmuir* **2009**, *25*, 12529.
- (68) Svensson, O.; Lindh, L.; Cardenas, M.; Arnebrant, T. *J. Colloid Interface Sci.* **2006**, *299*, 608.
- (69) Zembala, M.; Adamczyk, Z.; Kolasinska, M.; Warszynski, P. *Colloids Surf, A* **2007**, *302*, 455.
- (70) Vörös, J. *Biophys. J.* **2004**, *87*, 553.
- (71) Halthur, T. J.; Elofsson, U. M. *Langmuir* **2004**, *20*, 1739.
- (72) Iturri Ramos, J. J.; Stahl, S.; Richter, R. P.; Moya, S. E. *Macromolecules* **2010**, *43*, 9063.
- (73) Crouzier, T.; Boudou, T.; Picart, C. *Curr. Opin. Colloid Interface Sci.* **2010**, *15*, 417.
- (74) Wong, J. E.; Rehfeldt, F.; Hanni, P.; Tanaka, M.; Klitzing, R. V. *Macromolecules* **2004**, *37*, 7285.
- (75) Kujawa, P.; Moraille, P.; Sanchez, J.; Badia, A.; Winnik, F. *J. Am. Chem. Soc.* **2005**, *127*, 9224.
- (76) Larsson, R. G. *The Structure and Rheology of Complex Fluids*; Oxford University Press: Oxford, U.K., 1999.